

Dibenzothiazoles as novel amyloid-imaging agents

Chunying Wu,^{a,b} Jingjun Wei,^b Kuanqiang Gao^b and Yanming Wang^{a,b,*}

^aDepartment of Chemistry and Radiology, Case Western Reserve University, Cleveland, OH 44106, USA

^bCollege of Pharmacy, Department of Medicinal Chemistry and Pharmacognosy, University of Illinois at Chicago, Chicago, IL 60612, USA

Received 3 July 2006; revised 3 November 2006; accepted 13 November 2006

Available online 16 November 2006

Abstract—Novel dibenzothiazole derivatives were synthesized and evaluated as amyloid-imaging agents. In vitro quantitative binding studies using AD brain tissue homogenates showed that the dibenzothiazole derivatives displayed high binding affinities with K_i values in the nanomolar range (6.8–36 nM). These derivatives are relatively lipophilic with partition coefficients ($\log P_{oct}$) in the range of 1.25–3.05. Preliminary structure–activity relationship studies indicated dibenzothiazole derivatives bearing electron-donating groups exhibited higher binding affinities than those bearing electron-withdrawing groups. A lead compound was selected for its high binding affinity and radiolabeled with [¹²⁵I] through direct radioiodination using sodium [¹²⁵I] iodide in the presence of Chloramine T. The radioligand (4-[2,6']dibenzothiazolyl-2'-yl-2-[¹²⁵I]-phenylamine) displayed moderate lipophilicity ($\log P_{oct}$, 2.70), very good brain uptake ($3.71 \pm 0.63\%$ ID/g at 2 min after iv injection in mice), and rapid washout from normal brains (0.78% and 0.43% ID/g at 30 and 60 min, respectively). These studies indicated that lipophilic dibenzothiazole derivatives represent a promising pharmacophore for the development of novel amyloid-imaging agents for potential application in Alzheimer's disease and related neurodegenerative disorders.

© 2007 Elsevier Ltd. All rights reserved.

1. Introduction

Alzheimer's disease (AD) is a progressive and irreversible neurodegenerative disorder that is characteristic of amyloid deposition in the forms of senile plaques (SPs) and neurofibrillary tangles (NFTs).^{1–4} Both SP and NFT accumulation have been suggested as early and specific events in the pathogenesis of AD.^{5–8} Currently postmortem histopathological examination of SP and NFTs in the brain is still the only method for definitive diagnosis. One of the major tasks in AD research is to detect and quantify SP and NFT in living subjects, preferably at early or even pre-symptomatic stages. Toward this goal, nuclear imaging techniques such as positron emission tomography (PET) and single photon emission computed tomography (SPECT) have been employed. When used in conjunction with trace amount radioligands, PET and SPECT have the capacity to detect and quantify amyloid deposition in vivo. As a prerequisite to using these imaging techniques, amyloid-imaging

agents that readily enter the brain and specifically target at SP or NFTs have to be developed.

To date, applications of PET and SPECT for amyloid-imaging have been hampered by the lack of suitable amyloid-imaging probes. Recent efforts have been focused on small-molecule amyloid dyes used widely in AD pathology. Such amyloid dyes include Congo Red (CR), thioflavin T (ThT), and thioflavin S (ThS) (Fig. 1). Because these histological dyes are either positively or negatively charged, they are incapable of penetrating the brain–blood barrier (BBB). This has led to the development of neutral derivatives of the amyloid dyes for potential in vivo imaging studies.

Several types of amyloid-imaging agents have thus been synthesized and evaluated. Systematic modification of CR resulted in a series of bisstyrylbenzene derivatives.^{9–18} These bisstyrylbenzene derivatives exhibited high binding affinity and specificity with improved brain uptake. However, no lead compounds have been identified with in vivo pharmacokinetic profiles that meet a series of strict requirements set for in vivo imaging.

Further modification of CR also led to the design and synthesis of a series of stilbene derivatives as

Keywords: Amyloid- β ; Alzheimer's disease; Thioflavin S; PET; SPECT; Imaging.

* Corresponding author. Tel.: +1 216 844 3288; fax: +1 216 844 8062; e-mail: yanming.wang@case.edu

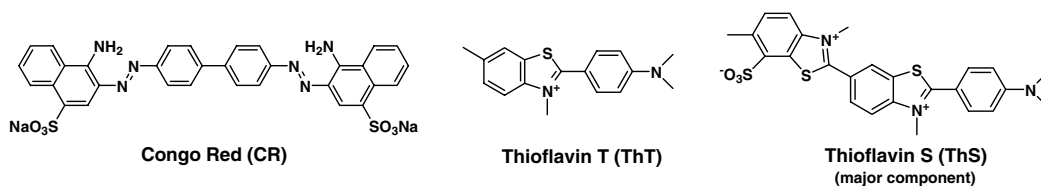


Figure 1. Structures of histological amyloid dyes used as prototypes for the development of amyloid-imaging agents.

amyloid-imaging agents for either PET or SPECT studies.^{19–25} Following appropriate radiolabeling, the stilbene derivatives have been evaluated for in vivo and in vitro binding properties to amyloid deposits and pharmacokinetic profiles. Most of these stilbene derivatives readily penetrated the BBB and selectively bound to amyloid deposits at high affinities. These studies have led to the identification of a lead compound, termed [¹¹C]SB-13 ([¹¹C]-4-*N*-methylamino-4'-hydroxystilbene) (Fig. 2), that can be used for PET amyloid-imaging in human subjects.²⁰ In AD subjects, [¹¹C]SB-13 displayed an accumulate pattern that is considered consistent with the previously reported AD pathology. In contrast, little or no retention of [¹¹C]SB-13 was observed in age-matched control subjects.²⁰

Another amyloid dye that has been extensively studied is thioflavin T (ThT). ThT is a positively charged histological dye for amyloid that cannot penetrate the BBB.²⁶ Elimination of the positive charge has led to the development of a series of benzothiazole and related heterocycles such as 2-aryl-substituted benzothiazole derivatives,^{17,27–31} 2-aryl-substituted benzoxazole derivatives,³² 2-aryl-substituted benzofuran,³³ and imidazo [1,2- α] pyridine derivatives.^{34,35} Most of these neutral, lipophilic ThT analogs bind to amyloid fibrils with high affinity and specificity. The in vivo pharmacokinetic profiles of the above heterocyclic compounds have been extensively evaluated as potential amyloid-imaging agents. Compared to neutral CR analogs, lipophilic ThT analogs have even smaller molecular weights and display a higher brain uptake. A lead compound, termed PIB ([¹¹C]-2-(4-(methylamino)phenyl)-6-hydroxybenzothiazole) (Fig. 2), was thus identified for human studies. Extensive clinical PET studies indicated that PIB readily entered the brain and selectively bound to amyloid deposits in AD subjects. PIB accumulation is predominant in the cortical areas known for amyloid deposition

in AD subjects. Conversely, PIB showed rapid entry and clearance in all cortical gray matter of healthy control subjects.

As an imaging agent for SPECT, a [¹²³I]-labeled imidazo [1,2- α] pyridine derivative, termed IMPY (6-iodo-2-(4'-dimethylamino)-phenyl-imidazo[1,2]pyridine) (Fig. 2), has been identified and its pharmacological effects have been evaluated in human subjects. Preliminary studies in both AD and normal control subjects demonstrated that IMPY is a safe radiotracer for clinical imaging studies.³⁶ These studies paved the way for the potential use of [¹²³I] IMPY in clinical SPECT imaging of amyloid deposits in human subjects.

In addition, amyloid-imaging agents have also been derived from other histological dyes such as acridine orange,^{37,38} fluorene,³⁹ and DDNP.^{40–42} In fact, the first PET amyloid-imaging studies in human subjects were carried out with a F-18-labeled DDNP analog termed [¹⁸F] FDDNP ([¹⁸F]-2-(1-(2-(*N*-(2-fluoroethyl)-*N*-methylamino) naphthalene-6-yl) ethylidene) malononitrile)⁴³ (Fig. 2). Clinical studies suggested that [¹⁸F]FDDNP's retention in amyloid deposit regions may be due to selective binding to both SPs and NFTs in the brain.

In this work, we report a series of dibenzothiazole derivatives as amyloid-imaging agents. The dibenzothiazole pharmacophore is seen in several histological dyes such as primuline⁴⁴ and thioflavin S (ThS).^{45–47} Primuline and ThS have been commonly used as viability stains of starch in phytoplankton and a fluorescent stain for amyloid, respectively. However, Primuline and ThS exist as a mixture of several components. The major component of these dyes contains two conjugated benzothiazole units.⁴⁸ We thus designed and synthesized a series of dibenzothiazole derivatives. Compared with primuline and ThS, these dibenzothiazole derivatives are lipophilic and readily enter the brain, making it possible for

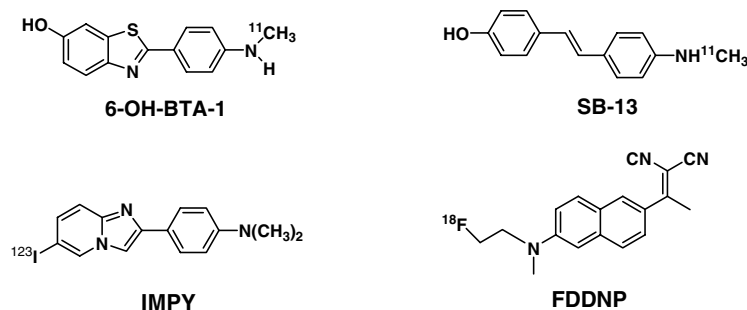


Figure 2. Structures of amyloid-imaging agents that have been evaluated in human subjects.

potential in vivo amyloid-imaging agents. In vitro evaluations suggested that these dibenzothiazole derivatives bound to amyloid deposits in AD brain homogenates with high affinities. In vivo brain permeability studies of selected compounds displayed high initial brain uptake. These studies thus expand the current portfolio of amyloid-imaging agents for potential clinical applications.

2. Results and discussion

2.1. Chemistry, synthesis, and radiolabeling

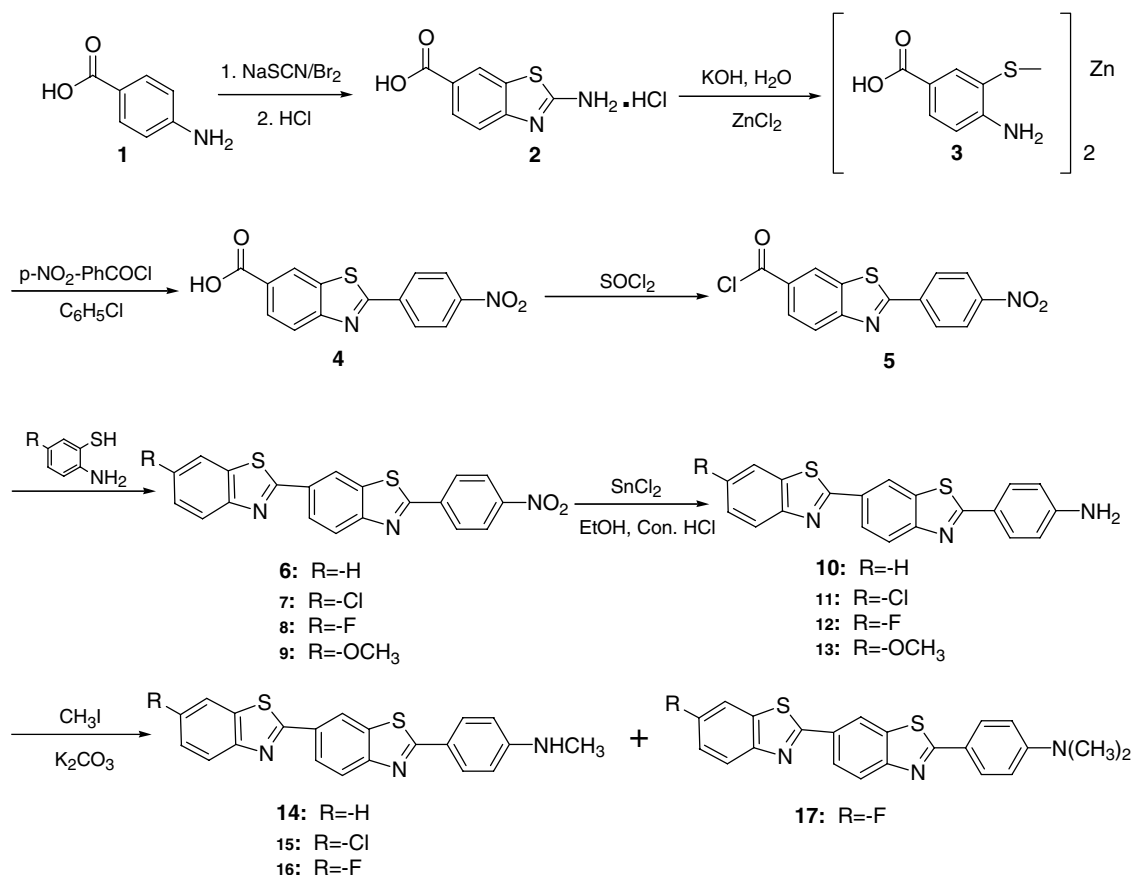
The synthesis of dibenzothiazole derivatives is described in Scheme 1 starting from commercially available *p*-aminobenzothiazole (**1**). As shown in Scheme 1, 2-aminobenzothiazole-6-carboxylic acid (**2**) was first prepared from **1** based on previously reported procedures.⁴⁹ Basic hydrolysis of **2** followed by neutralizing in HCl and ZnCl₂ yielded the Zinc salt of 4-amino-3-mercaptobenzoic acid (**3**), which was coupled immediately with *p*-nitrobenzoyl chloride to give 2-(4-nitro-phenyl)-benzothiazole-6-carboxylic acid (**4**) with 83% yield. The 6-carboxylic acid of **4** was then converted into acyl chloride (**5**) followed by coupling with a 5-substituted amino-phenol to give 6''-substitute-2'-(4-nitro-phenyl)-[2,6']dibenzothiazolyl (**6–9**). Reduction of **6–9** with SnCl₂ in ethanol afforded 6''-substitute-2'-([2,6']dibenzothiazolyl-2'-yl)-aniline (**10–13**), which can be further

methylated with methyl iodide and K₂CO₃ in DMSO to monomethylamino derivatives (**14–16**) and dimethylamino derivatives (**17**).

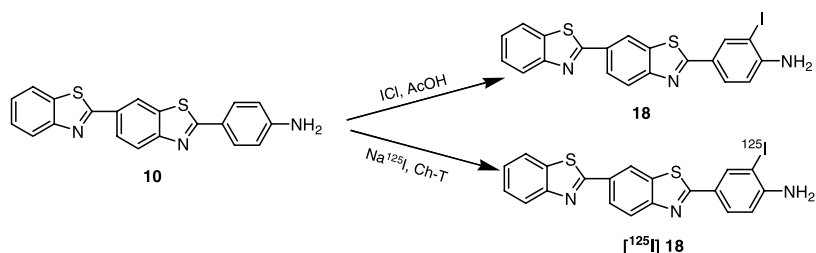
The synthesis of an iodinated compound 4-[2,6']dibenzothiazolyl-2'-yl-2-iodo-phenylamine (**18**) and its radiolabeling with ¹²⁵I is described in Scheme 2. Thus, the cold standard compound **18** was first synthesized by treating **10** with ICl in AcOH at room temperature for 18 h. Similarly, compound **10** was also used directly as the precursor for radiolabeling. This synthesis of [¹²⁵I] **18** was achieved through direct radioiodination using sodium [¹²⁵I] iodide in the presence of Chloramine T (ChT). The reaction was monitored by HPLC and went to completion after 3 h. The overall radiochemical yields of [¹²⁵I] **18** were 20–30% after HPLC purification. [¹²⁵I] **18** was obtained with a radiochemical purity over 98% and a specific activity near the theoretical limit (80 TBq/mmol) based on the no-carrier added sodium [¹²⁵I] iodide. The radiochemical identity of [¹²⁵I] **18** was verified by co-elution with the non-radioactive cold standard **18** on HPLC profiles. [¹²⁵I] **18** was stable enough to be kept for up to 8 h at room temperature and for up to 2 months in the refrigerator.

2.2. Partition coefficients

Based on the conventional octanol–water partition measurement, the lipophilicity of [¹²⁵I] **18** was determined in terms of partition coefficients (logP oct).



Scheme 1. Synthesis of dibenzothiazole derivatives.



Scheme 2. Synthesis and [¹²⁵I] labeling of **18**.

The logP oct of [¹²⁵I] **18** was found at 2.70 and the logP oct values of other dibenzothiazole derivatives were then estimated based on coefficients determined by Hansch and Leo⁵⁰ As shown in Figure 3, the logP oct values of these derivatives are between 1 and 3, a range that has been previously proposed for optimal brain uptake.⁵¹

2.3. In vitro quantitative binding assay using AD brain region homogenates

The binding affinities of these newly developed compounds for β -amyloid were evaluated using AD brain homogenates and tritiated PIB ([³H]PIB, Amersham), a radioligand previously developed with a high affinity for synthetic A β aggregation ($K_i = 4.3$ nM).³⁰ The post-mortem brain tissues were obtained from well-defined AD patients. The gray matter was then carefully separated from white matter at autopsy and kept in -70 °C. The fresh frozen gray matter was then homogenized by milling it thoroughly in a mortar in the presence of liquid nitrogen. The homogenates were then prepared in phosphate-buffered saline (PBS, pH 7.4) at a concentration of approximately 400 mg tissue/ml,

aliquoted into 1-ml portions, and stored at -70 °C for future use.

As shown in Figure 3, the newly developed dibenzothiazole derivatives competed effectively with [³H]PIB binding site(s) on AD homogenates at high affinities, the K_i values of compounds **10–18** are shown in Figure 3, which showed relatively high binding affinities in the range of 6.8–36 nM. The results indicated that these dibenzothiazole derivatives bind to the same site as PIB does on AD homogenates. According to the in vitro binding assays, functional groups have moderate effects on the binding affinity. Compounds containing electron-donating groups showed slightly higher binding affinity than those containing electron-withdrawing group. For example, the K_i values decreased in the order of **12** (6-F) > **11** (6-Cl) > **10** (6-H) > **PIB** (6-OH), consistent with the order of increasing electron-donating capacity. In addition, methylation of the amino group increased the binding affinity. Thus, *N,N*-dimethylated derivative (compound **17**) and *N*-monomethylated derivatives (compounds **14–16**) displayed higher binding affinities than that of the primary amino derivatives (compounds **10–13**).

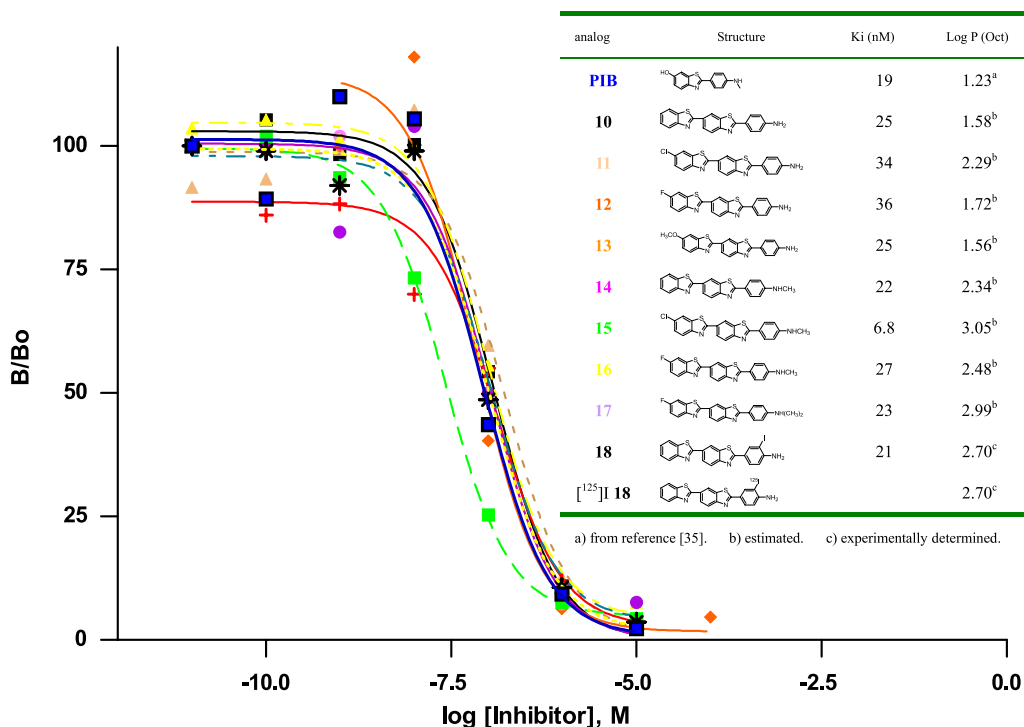


Figure 3. Competitive binding assays of dibenzothiazole derivatives using [³H] PIB as the radioligand in AD brain tissue homogenates, and the binding affinity (K_i) and lipophilicity (logP oct) of newly synthesized dibenzothiazole derivatives.

Table 1. Brain uptake in mice ($n = 3$, %ID/g)

| Compound | 2 min | 30 min | 60 min |
|-------------------------------|-------------|-------------|-------------|
| [¹²⁵ I] 18 | 3.71 ± 0.63 | 0.78 ± 0.14 | 0.43 ± 0.12 |

2.4. In vivo brain uptake in normal mice

For potential in vivo imaging studies, we radiolabeled compound **10** with ¹²⁵I for brain uptake studies. Following a single iv injection of [¹²⁵I] **18** (0.2 ml, 0.185 MBq), the brain permeability was evaluated in normal mice. The brain radioactivity concentration of [¹²⁵I] **18** was determined at 2, 30, and 60 min postinjection. As shown in Table 1, [¹²⁵I] **18** displayed rapid brain entry at early time intervals. The initial brain uptake was 3.71 ± 0.63% ID/g at 2 min postinjection, a level that is considered for potential clinical imaging studies. The brain radioactivity concentration decreased sharply to 0.78 ± 0.14% ID/g at 30 min and 0.43 ± 0.12% ID/g at 60 min, with a 2-to-30 min ratio of 5. These results indicate that the non-specific binding of [¹²⁵I] **18** was just as low as it rapidly clears from the normal mouse brain in the absence of amyloid deposits.

3. Conclusion

In summary, we have developed a new type of amyloid-imaging agent based on the dibenzothiazole pharmacophore. These derivatives displayed high binding affinities for AD brain homogenates. When labelled with ¹²⁵I, [¹²⁵I] **18** readily enters the brain at early time intervals followed by rapid washout from the normal mouse brain, indicating low non-specific binding. Further studies are under way to systematically evaluate these novel amyloid-imaging agents for potential in vivo studies. Once fully developed, these agents would allow for an early detection and quantification of the amyloid load in living subjects and facilitate efficacy in evaluating anti-amyloid therapies currently being investigated.^{52,53}

4. Experimental

4.1. General remarks

All chemicals were purchased from Sigma-Aldrich and used without further purification. ¹H NMR spectra were obtained at 300 MHz on Bruker DPX-300 (QNP probe) NMR spectrometers using 5 mm NMR tubes (Wilmad 528-PP) in CDCl₃ or DMSO-*d*₆ (Aldrich or Cambridge Isotopes) solutions at room temperature. Chemical shifts are reported as δ values relative to internal TMS. HR-ESIMS were acquired under the electron spray ionization (ESI) condition. The radioactivities of ¹²⁵I and ³H were calculated by the counts per minute in a γ counter (Cobra Packard model U5005) and a multiple-purpose scintillation counter (Beckman, LS 6500). Radiochemical purity was determined by Hewlett Packard high-pressure liquid chromatography (HPLC) system equipped with UV and Bioscan flow count detectors.

4.2. Synthesis of 2-aminobenzothiazole-6-carboxylic acid (**2**)⁴⁹

NaSCN (65 g, 0.8 mol) was added to a suspension of commercially available 4-amino-benzoic acid (**1**, 100 g, 0.73 mol) in MeOH followed by the addition of Br₂ (38 ml, 0.73 mol) in portions. The above solution was allowed to cool to −10 °C and stirred for 2 h while keeping the inner temperature below −5 °C. The precipitate was then filtered and suspended in 350 ml of 1 M HCl. The suspension was heated to reflux for 30 min. After immediate filtration, 150 ml concd HCl was added to the hot filtrate to give 70 g (yield 42%) of 2-amino-benzothiazole-6-carboxylic acid (**2**) (as a white solid), which was dried and used without further purification.

4.3. Synthesis of Zinc salt of 4-amino-3-mercaptopbenzoic acid (**3**)

Under Argon, compound **2** (9.18 g, 40 mmol) was dissolved in a KOH solution (45 g KOH/45 ml water) and heated to reflux for 3 h. After being cooled to room temperature, the solution was neutralized by concd HCl (50 ml). Then ZnCl₂ in 25 ml of water was added slowly while white solid precipitated out. The suspension was acidified by AcOH. The solid was filtered, washed with water, and dried in a vacuum to give 8.18 g (98 %) of 4-amino-3-mercaptopbenzoic acid (**3**) as a white solid. ¹H NMR (300 MHz, DMSO-*d*₆) δ 12.02 (br, 2H), 7.90 (s, 1H), 7.63 (d, *J* = 7.0 Hz, 1H), 7.53 (s, 1H), 7.30 (d, *J* = 8.0 Hz, 1H), 6.74 (d, *J* = 8.5 Hz, 1H), 6.55 (d, *J* = 8.1 Hz, 1H), 6.24 (br, 2H), 5.66 (br, 2H).

4.4. Synthesis of 2-(4'-nitrophenyl)-6-(benzothiazol-yl)benzothiazole (**4**)

Compound **3** (8.18 g, 20 mmol) was suspended in pyridine (50 ml) and heated to 80 °C. *p*-Nitrobenzoyl chloride (7.95 g, 42.8 mmol) was added in portions to give a clear solution, which was stirred for another hour. After being cooled to room temperature, the precipitate was filtered, washed with dilute hydrochloric acid and water, and dried under a vacuum to afford 9.95 g (83%) of 2-(4'-nitrophenyl)-6-(benzothiazolyl)benzothiazole (**4**), which was used directly without further purification.

4.5. Synthesis of 2-(4-nitro-phenyl)-benzothiazole-6-carbonyl chloride (**5**)

Compound **4** (1.00 g, 3.3 mmol) was suspended in SOCl₂ (5 ml) and heated to reflux for 1 h. Then excess SOCl₂ was evaporated under reduced pressure to get 2-(4-nitro-phenyl)-benzothiazole-6-carbonyl chloride (**5**), which was used without further purification.

4.6. General synthesis of 6'-substitute-2'-(4-nitro-phenyl)-[2,6']dibenzothiazolyl (**6–9**)

To a suspension of **5** in chlorobenzene (28 ml), 5-substituted aminothiophenol (2-aminothiaphenol (0.60 g, 4.8 mmol), 2-amino-5-chloro-benzenethiol (0.60 g, 3.75 mmol), 2-amino-5-fluoro-benzenethiol (0.60 g,

4.2 mmol), and 2-amino-5-methoxy-benzenethiol (0.65 g, 4.19 mmol) were added, respectively. The obtained mixtures were heated to reflux for 3 h. After being cooled to room temperature, the solids were filtered and dried under vacuum to give **6** (1.00 g, 79%), **7** (1.00 g, 73%), **8** (1.03 g, 76%), and **9** (1.02 g, 74%).

4.7. General synthesis of 4-(6-substitute-[2,6']dibenzothiazolyl-2'-yl)-phenylamine (10–13)

To a suspension of **6–9** in concd HCl (13 ml), ethanol (100 ml), and SnCl₂ (2.00 g, 10.0 mmol) were added. The suspension was heated to 80 °C for 1 h. After being cooled to room temperature; the solid was filtered; washed with concentrated HCl, water, and dilute ammonium; and dried in vacuum to give **10** (0.88 g, quant.), ¹H NMR (300 MHz, DMSO-*d*₆) δ 8.82 (d, *J* = 1.5 Hz, 1H), 8.18 (d, *J* = 8.5 Hz, 2H), 8.08 (d, *J* = 8.0 Hz, 1H), 8.03 (d, *J* = 8.5 Hz, 1H), 7.82 (d, *J* = 8.5 Hz, 2H), 7.57 (t, *J* = 7.3 Hz, 1H), 7.48 (t, *J* = 7.3 Hz, 1H), 6.69 (d, *J* = 8.5 Hz, 2H), 6.03 (s, 2H). HR-ESIMS: *m/z* calcd for C₂₀H₁₄N₃S₂ (M+H⁺): 360.0629, found 360.0631. Compound **11** (0.9 g, quant.), ¹H NMR (300 MHz, DMSO-*d*₆) δ 8.82 (s, 1H), 8.35 (s, 1H), 8.18 (d, *J* = 4.4 Hz, 2H), 8.06 (t, *J* = 8.8 Hz, 2H), 7.81 (d, *J* = 8.5 Hz, 2H), 7.60 (d, *J* = 4.3 Hz, 1H), 6.71 (d, *J* = 8.5 Hz, 2H), 6.04 (s, 1H). HR-ESIMS: *m/z* calcd for C₂₀H₁₂ClN₃S₂ (M+H⁺): 394.0239, found 394.0225. Compound **12** (0.83 g, quant.), ¹H NMR (400 MHz, DMSO-*d*₆) δ 8.80 (d, *J* = 6.3 Hz, 1H), 8.01–8.18 (m, 6H), 7.83 (d, *J* = 7.4 Hz, 2H), 7.44 (d, *J* = 4.6 Hz, 1H), 6.71 (d, *J* = 7.7 Hz, 2H). HR-ESIMS: *m/z* calcd for C₂₀H₁₂FN₃S₂ (M+H⁺): 378.0535, found 378.0523. Compound **13** (1.03 g, quant.), ¹H NMR (400 MHz, DMSO-*d*₆) δ 8.43 (d, *J* = 2.9 Hz, 1H), 7.98 (dd, *J* = 6.9, 8.7 Hz, 2H), 7.80 (t, *J* = 8.6 Hz, 2H), 7.14 (m, 3H), 6.69 (d, *J* = 8.6 Hz, 2H), 6.02 (s, 2H), 3.87 (s, 3H). HR-ESIMS: *m/z* calcd for C₂₁H₁₅N₃OS₂ (M+H⁺): 390.0735, found 390.0728.

4.8. General synthesis of [4-(6-substitute-[2,6']dibenzothiazolyl-2'-yl)-phenyl]-methylamine (14–15)

Under Argon, compounds **10–11** (1.30 mmol) and K₂CO₃ (1.15 g, 8.34 mmol) were suspended in DMSO (15 ml) followed by an addition of MeI (0.17 ml, 2.78 mmol). The sealed vial was heated to 100 °C and stirred for 31 h. The solution was diluted with ethyl acetate and washed with water and brine, and dried over Na₂SO₄. After evaporating the solvent, the crude product was purified by flash column chromatography (hexane/ethyl acetate = 4:1–2:1) to give **14** (36 mg, 7%). ¹H NMR (300 MHz, DMSO-*d*₆) δ 8.83 (s, 1H), 8.18 (d, *J* = 8.0 Hz, 2H), 8.08 (d, *J* = 8.0 Hz, 1H), 8.04 (d, *J* = 8.5 Hz, 1H), 7.88 (d, *J* = 8.6 Hz, 1H), 7.55 (t, *J* = 7.0 Hz, 1H), 7.46 (t, *J* = 7.0 Hz, 1H), 6.69 (d, *J* = 8.6 Hz, 2H), 6.62 (d, *J* = 5.1 Hz, 1H), 2.78 (d, *J* = 5.1 Hz, 3H). HR-ESIMS: *m/z* calcd for C₂₁H₁₆N₃S₂ (M+H⁺): 374.0786, found 374.0797. Compound **15** (100 mg, 19%). ¹H NMR (300 MHz, DMSO-*d*₆) δ 8.82 (s, 1H), 8.35 (s, 1H), 8.18 (d, *J* = 4.3 Hz, 1H), 8.05 (t, *J* = 8.7 Hz, 2H), 7.81 (d, *J* = 8.7 Hz, 2H), 7.61 (d, *J* = 4.4 Hz, 1H), 6.68 (d,

J = 8.8 Hz, 2H), 6.63 (s, 1H), 2.79 (s, 3H). HR-ESIMS: *m/z* calcd for C₂₁H₁₄ClN₃S₂ (M+H⁺): 408.0396, found 408.0382.

4.9. Synthesis of [4-(6-fluoro-[2,6']dibenzothiazolyl-2'-yl)-phenyl]-methylamine (16) and [4-(6-fluoro-[2,6']dibenzothiazolyl-2'-yl)-phenyl]-dimethylamine (17)

Under Argon, the compound **12** (0.50 g, 1.32 mmol) and K₂CO₃ (1.10 g, 6 mmol) were suspended in DMSO (15 ml) and MeI (0.17 ml, 2.78 mmol) was added. The sealed vial was heated to 100 °C and stirred for 31 h. The solution was diluted with ethyl acetate and washed with water and brine, dried on Na₂SO₄, concentrated, and purified by column chromatography (hexane/ethyl acetate = 4:1–2:1) to give compound **16** (58 mg, 22%) and compound **17** (91 mg, 34%). Compound **16**: ¹H NMR (400 MHz, DMSO-*d*₆) δ 8.38 (s, 1H), 7.95–8.21 (m, 4H), 7.87 (d, *J* = 7.3 Hz, 2H), 7.44 (d, *J* = 4.5 Hz, 1H), 6.69 (d, *J* = 7.6 Hz, 2H), 2.38 (s, 3H). HR-ESIMS: *m/z* calcd for C₂₁H₁₄FN₃S₂ (M+H⁺): 392.0691, found 392.0680. Compound **17**: ¹H NMR (400 MHz, DMSO-*d*₆) δ 8.42 (s, 1H), 8.00–8.20 (m, 4H), 7.79 (d, *J* = 7.3 Hz, 2H), 7.45 (d, *J* = 4.5 Hz, 1H), 6.70 (d, *J* = 7.5 Hz, 2H), 2.44 (s, 6H). HR-ESIMS: *m/z* calcd for C₂₂H₁₆FN₃S₂ (M+H⁺): 406.0848, found 406.0844.

4.10. Synthesis of 4-[2,6']dibenzothiazolyl-2'-yl-2-iodo-phenylamine (18)

Under Argon, ICl (0.07 ml) was added dropwise to the suspension of **10** (20 mg, 0.056 mM) in AcOH (10 ml). The resulting mixture was sealed and stirred at room temperature for 18 h. The reaction was quenched with ethanol and the solvent was removed. The residue was purified by preparative TLC to get 4-[2,6']dibenzothiazolyl-2'-yl-2-iodo-phenylamine (**18**, 10 mg, 38%) as brown solid. ¹H NMR (300 MHz, DMSO-*d*₆) δ 8.87 (s, 1H), 8.44 (s, 1H), 8.40 (d, *J* = 3.6 Hz, 1H), 8.32 (d, *J* = 1.8 Hz, 1H), 7.82 (d, *J* = 8.5 Hz, 2H), 7.64 (s, 1H), 7.57 (t, *J* = 7.3 Hz, 1H), 7.48 (t, *J* = 7.3 Hz, 2H), 6.69 (d, *J* = 8.5 Hz, 1H), 6.10 (s, 1H). HR-ESIMS: *m/z* calcd for C₂₀H₁₂IN₃S₂ (M+H⁺): 485.9596, found 485.9588.

4.11. Synthesis of 4-[2,6']dibenzothiazolyl-2'-yl-2-¹²⁵I-phenylamine (¹²⁵I) **18**

To a solution of **10** (1 mg) in 1 ml acetic acid was added sodium [¹²⁵I]iodide (specific activity 83.05 TBq/mmol) in 0.01 M sodium hydroxide solution. Following the addition of 50 μl Chloramine T solution (ChT, 30 mg dissolved in 500 μl acetic acid), the reaction mixture was stirred at room temperature for 3 h, and quenched with 200 μl/L sodium hydrogensulfite (1 M) solution. The mixture was diluted with 20 ml of water and adjusted to pH 7–8 with saturated NaHCO₃. The reaction mixture was then loaded onto a Waters C-8 Sep-Pak™ plus cartridge. The Sep-Pak cartridge was washed with 10 ml of water and dried with a rapid air bolus, and the radioiodinated product was slowly eluted with 2 ml of methanol. The solution was concentrated under nitrogen to about 200 μl and the crude product was purified by HPLC using a Phenomenex C-18 column

(250 × 4.6 mm, acetonitrile:TEA buffer (pH 7.5) = 85:15, flow rate 1.0 ml/min, t_R = 17.31 min). The desired fractions were collected, diluted with 50 ml of water, and loaded onto a water C-8 Sep-Pak™ plus cartridge. After being washed with another 10 ml of water and dried with a rapid air bolus, the cartridge was eluted with 2 ml ethanol and dried under N₂ to give the final product [¹²⁵I] **18** in overall 20–30% radiochemical yields with radiochemical purities of >98% after purification by HPLC.

4.12. Partition coefficient determination

Partition coefficients were measured by mixing [¹²⁵I] **18** (10 μl, RCP > 98%, approximately 50,000 cpm) with sodium phosphate buffer (PBS, 3 g, 0.1 M, pH 7.4) and *n*-octanol (3 g, 3.65 ml) in test tubes. The tubes were vortexed for 3 min (1 min 3×) at room temperature followed by centrifugation at 3500 rpm for 5 min. Then 1 ml of buffer and 1 ml of *n*-octanol were taken out, weighed, and counted. The partition coefficient was determined by calculating the ratio of cpm/g of *n*-octanol to that of PBS and expressed as logP_{oct} = log [cpm/g (*n*-octanol)/cpm/g(PBS)]. Another 2 ml from the rest of *n*-octanol layer was taken out and repartitioned in a tube previously containing 3 g PBS and 1.65 ml of *n*-octanol until consistent partitions of the coefficient values were obtained. All assays were performed in triplicate.

4.13. Quantitation of [¹²⁵I] **18** in mice brain

The radiolabeled ligand [¹²⁵I] **18** eluted from C-18 Sep-Pak™ plus cartridge was dissolved in a mixture consisting of saline (2 ml, 9 mg/ml), ethylene glycol (2 ml), ethanol (0.7 ml), and HCl (0.3 ml, 0.3 nM). Under anesthesia, 0.1 ml of the above solution containing 0.185 MBq of radioactive tracer was administered to the mice through a tail vein injection (Swiss-Webster, *n* = 3, 2 months old). The mice were then sacrificed by a heart puncture at 2, 30, and 60 min postinjection. The brain was rapidly removed, weighed, and counted. The uptake of brain was expressed as percentage of injection dose per gram.

4.14. In vitro binding to AD homogenates

Binding was assayed in 12 × 75 mm borosilicate glass tubes. For saturation studies, the reaction mixture contained 50 μl of AD homogenates (10–50 μg), 50 μl of [³H]PIB (diluted in PBS, 0.1–1 nM), and 50 μl of cold PIB (10 μM, diluted in PBS containing DMSO (less than 1%)) in a final volume of 500 μl. Nonspecific binding was defined in the presence of 10 μM cold standard PIB in the same assay tubes. For competition binding, the reaction mixture contained 50 μl AD homogenates, inhibitors [10⁻⁵–10⁻¹² mol/L in PBS containing DMSO (less than 1%)], [³H]PIB (in PBS, 0.05 nM in the final mixture), and PBS (10 mM) in a final volume of 500 μl. The resulting mixture was incubated at 37 °C for 1 h, and the bound and free radioligands were separated by rapid vacuum filtration through Whatman GF/B glass filter

paper using a Brandel M-24R cell harvest and rapidly washed three times at room temperature with PBS. The filters containing the bound radioactivity were transferred to special vials containing 3 ml of universal scintillation fluid. Vials were counted using Beckman LS6500 multi-purpose scintillation counter. Specific binding was estimated as the difference between total and nonspecific binding. Under the assay conditions, the specifically bound fraction was less than 15% of the total radioactivity. The results were subjected to nonlinear regression analysis using software GraphPad Prism by which K_d and K_i values were calculated.

Acknowledgments

We thank Dr. Anil Gulati (University of Illinois at Chicago) for assistance in the in vitro binding assays. This work was supported in part by grants from the Alzheimer's Association, the Institute for the Study of Aging (Y.W.), and the National Institute on Aging (AG22048, Y.M.). This work was also supported by National Natural Science Foundation of P.R. China (30470496, C. Wu) and Natural Science Foundation of Jiangsu Province, P.R. China (BK2004-423, C. Wu).

References and notes

- Hardy, J. A.; Higgins, G. A. *Science* **1992**, *256*, 184–185.
- Hardy, J.; Selkoe, D. J. *Science* **2002**, *297*, 353–356.
- Braak, H.; Braak, E. *J. Neural. Transm. Suppl.* **1998**, *53*, 127–140.
- Trojanowski, J. Q.; Clark, C. M.; Schmidt, M. L.; Arnold, S. E.; Lee, V. M. *Neurobiol. Aging* **1997**, *18*, S75–S79.
- Selkoe, D. J. *Ann. N.Y. Acad. Sci.* **2000**, *924*, 17–25.
- Naslund, J.; Haroutunian, V.; Mohs, R.; Davis, K. L.; Davies, P.; Greengard, P.; Buxbaum, J. D. *JAMA* **2000**, *283*, 1571–1577.
- Selkoe, D. J. *JAMA* **2000**, *283*, 1615–1617.
- Manczak, M.; Anekonda, T. S.; Henson, E.; Park, B. S.; Quinn, J.; Reddy, P. H. *Hum. Mol. Genet.* **2006**, *15*, 1437–1449.
- Klunk, W. E.; Debnath, M. L.; Pettegrew, J. W. *Neurobiol. Aging* **1995**, *16*, 541–548.
- Styren, S. D.; Hamilton, R. L.; Styren, G. C.; Klunk, W. E. *J. Histochem. Cytochem.* **2000**, *48*, 1223–1232.
- Link, C. D.; Johnson, C. J.; Fonte, V.; Paupard, M.; Hall, D. H.; Styren, S.; Mathis, C. A.; Klunk, W. E. *Neurobiol. Aging* **2001**, *22*, 217–226.
- Ishii, K.; Klunk, W. E.; Arawaka, S.; Debnath, M. L.; Furiya, Y.; Sahara, N.; Shoji, S.; Tamaoka, A.; Pettegrew, J. W.; Mori, H. *Neurosci. Lett.* **2002**, *333*, 5–8.
- Mathis, C. A.; Wang, Y.; Klunk, W. E. *Curr. Pharm. Des.* **2004**, *10*, 1469–1492.
- Han, H.; Cho, C. G.; Lansbury, P. T., Jr. *J. Am. Chem. Soc.* **1996**, *118*, 4506–4507.
- Zhen, W.; Han, H.; Anguiano, M.; Lemere, C. A.; Cho, C. G.; Lansbury, P. T., Jr. *J. Med. Chem.* **1999**, *42*, 2805–2815.
- Dezutter, N. A.; Dom, R. J.; de Groot, T. J.; Bormans, G. M.; Verbruggen, A. M. *Eur. J. Nucl. Med.* **1999**, *26*, 1392–1399.
- Zhuang, Z. P.; Kung, M. P.; Hou, C.; Skovronsky, D. M.; Gur, T. L.; Plossl, K.; Trojanowski, J. Q.; Lee, V. M.; Kung, H. F. *J. Med. Chem.* **2001**, *44*, 1905–1914.

18. Lee, H. J.; Zhang, Y.; Zhu, C.; Duff, K.; Pardridge, W. M. *J. Cereb. Blood Flow Metab.* **2002**, *22*, 223–231.
19. Zhuang, Z. P.; Kung, M. P.; Hou, C.; Plossl, K.; Kung, H. F. *Nucl. Med. Biol.* **2005**, *32*, 171–184.
20. Verhoeff, N. P.; Wilson, A. A.; Takeshita, S.; Trop, L.; Hussey, D.; Singh, K.; Kung, H. F.; Kung, M. P.; Houle, S. *Am. J. Geriatr. Psychiatry* **2004**, *12*, 584–595.
21. Ono, M.; Wilson, A.; Nobrega, J.; Westaway, D.; Verhoeff, P.; Zhuang, Z. P.; Kung, M. P.; Kung, H. F. *Nucl. Med. Biol.* **2003**, *30*, 565–571.
22. Ono, M.; Haratake, M.; Nakayama, M.; Kaneko, Y.; Kawabata, K.; Mori, H.; Kung, M. P.; Kung, H. F. *Nucl. Med. Biol.* **2005**, *32*, 329–335.
23. Kung, H. F.; Lee, C. W.; Zhuang, Z. P.; Kung, M. P.; Hou, C.; Plossl, K. *J. Am. Chem. Soc.* **2001**, *123*, 12740–12741.
24. Zhang, W.; Oya, S.; Kung, M. P.; Hou, C.; Maier, D. L.; Kung, H. F. *Nucl. Med. Biol.* **2005**, *32*, 799–809.
25. Zhang, W.; Oya, S.; Kung, M. P.; Hou, C.; Maier, D. L.; Kung, H. F. *J. Med. Chem.* **2005**, *48*, 5980–5988.
26. Burns, J.; Pennock, C. A.; Stoward, P. J. *J. Pathol. Bacteriol.* **1967**, *94*, 337–344.
27. Mathis, C. A.; Wang, Y.; Holt, D. P.; Huang, G. F.; Debnath, M. L.; Klunk, W. E. *J. Med. Chem.* **2003**, *46*, 2740–2754.
28. Mathis, C. A.; Bacskai, B. J.; Kajdasz, S. T.; McLellan, M. E.; Frosch, M. P.; Hyman, B. T.; Holt, D. P.; Wang, Y.; Huang, G. F.; Debnath, M. L.; Klunk, W. E. *Bioorg. Med. Chem. Lett.* **2002**, *12*, 295–298.
29. Wang, Y.; Klunk, W. E.; Debnath, M. L.; Huang, G. F.; Holt, D. P.; Shao, L.; Mathis, C. A. *J. Mol. Neurosci.* **2004**, *24*, 55–62.
30. Wang, Y.; Mathis, C. A.; Huang, G. F.; Debnath, M. L.; Holt, D. P.; Shao, L.; Klunk, W. E. *J. Mol. Neurosci.* **2003**, *20*, 255–260.
31. Wang, Y.; Klunk, W. E.; Huang, G. F.; Debnath, M. L.; Holt, D. P.; Mathis, C. A. *J. Mol. Neurosci.* **2002**, *19*, 11–16.
32. Zhuang, Z. P.; Kung, M. P.; Hou, C.; Plossl, K.; Skovronsky, D.; Gur, T. L.; Trojanowski, J. Q.; Lee, V. M.; Kung, H. F. *Nucl. Med. Biol.* **2001**, *28*, 887–894.
33. Ono, M.; Kung, M. P.; Hou, C.; Kung, H. F. *Nucl. Med. Biol.* **2002**, *29*, 633–642.
34. Zhuang, Z. P.; Kung, M. P.; Wilson, A.; Lee, C. W.; Plossl, K.; Hou, C.; Holtzman, D. M.; Kung, H. F. *J. Med. Chem.* **2003**, *46*, 237–243.
35. Cai, L.; Chin, F. T.; Pike, V. W.; Toyama, H.; Liow, J. S.; Zoghbi, S. S.; Modell, K.; Briard, E.; Shetty, H. U.; Sinclair, K.; Donohue, S.; Tipre, D.; Kung, M. P.; Dagostin, C.; Widdowson, D. A.; Green, M.; Gao, W.; Herman, M. M.; Ichise, M.; Innis, R. B. *J. Med. Chem.* **2004**, *47*, 2208–2218.
36. Newberg, A. B.; Wintering, N. A.; Plossl, K.; Hochold, J.; Stabin, M. G.; Watson, M.; Skovronsky, D.; Clark, C. M.; Kung, M. P.; Kung, H. F. *J. Nucl. Med.* **2006**, *47*, 748–754.
37. Suemoto, T.; Okamura, N.; Shiomitsu, T.; Suzuki, M.; Shimadzu, H.; Akatsu, H.; Yamamoto, T.; Kudo, Y.; Sawada, T. *Neurosci. Res.* **2004**, *48*, 65–74.
38. Shimadzu, H.; Suemoto, T.; Suzuki, M.; Shiomitsu, T.; Okamura, N.; Kudo, Y.; Sawada, T. *J. Label Compd. Radiopharm.* **2003**, *46*, 765–772.
39. Lee, C. W.; Kung, M. P.; Hou, C.; Kung, H. F. *Nucl. Med. Biol.* **2003**, *30*, 573–580.
40. Agdeppa, E. D.; Kepe, V.; Liu, J.; Flores-Torres, S.; Satyamurthy, N.; Petric, A.; Cole, G. M.; Small, G. W.; Huang, S. C.; Barrio, J. R. *J. Neurosci.* **2001**, *21*, RC189.
41. Agdeppa, E. D.; Kepe, V.; Petri, A.; Satyamurthy, N.; Liu, J.; Huang, S. C.; Small, G. W.; Cole, G. M.; Barrio, J. R. *Neuroscience* **2003**, *117*, 723–730.
42. Jacobson, A.; Petric, A.; Hogenkamp, D.; Sinur, A.; Barrio, J. R. *J. Am. Chem. Soc.* **1996**, *118*, 5572–5579.
43. Shoghi-Jadid, K.; Small, G. W.; Agdeppa, E. D.; Kepe, V.; Ercoli, L. M.; Siddarth, P.; Read, S.; Satyamurthy, N.; Petric, A.; Huang, S. C.; Barrio, J. R. *Am. J. Geriatr. Psychiatry* **2002**, *10*, 24–35.
44. Klut, M. E.; Stockner, J.; Bisalputra, T. *Histochem. J.* **1989**, *21*, 645–650.
45. Churukian, C. J.; Frank, M.; Horobin, R. W. *Biotech. Histochem.* **2000**, *75*, 147–150.
46. Westermark, G. T.; Johnson, K. H.; Westermark, P. *Methods Enzymol.* **1999**, *309*, 3–25.
47. Bancroft, J.; Gamble, M. *Theory and Practice of Histological Techniques*, 5th ed.; Churchill-Livingstone: London, 2002.
48. *Colour Index*, 3rd ed.; Society of Dyers and Colourists, American Association of Textile Chemists and Colorists: Bradford, 1971.
49. Schubert, V. M. *Justus Liebigs Ann. Chem.* **1947**, *558*, 10.
50. Hansch, C.; Leo, A. *Substituent Constants for Correlation Analysis in Chemistry and Biology*, 1st ed.; John Wiley and Sons: New York, 1979.
51. Wu, C.; Pike, V. W.; Wang, Y. *Curr. Top. Dev. Biol.* **2005**, *70*, 171–213.
52. Nordberg, A. *Lancet Neurol.* **2004**, *3*, 519–527.
53. Selkoe, D. J. *Nat. Biotechnol.* **2000**, *18*, 823–824.